Resonant four-wave parametric interactions: Adiabatic formulation

T. A. DeTemple, M. K. Gurnick, and F. H. Julien*

*Department of Electrical and Computer Engineering, University of Illinois at Urbana-Champaign,
1406 West Green Street, Urbana, Illinois 61801-2991*

The density-matrix approach, in the quasistatic or adiabatic limit, is applied to the case of resonant four-wave interactions in four-level systems resulting in explicit analytical expressions for the nonlinear optical parametric and nonparametric polarizations, including ac Stark effects. The results are applicable to any closed-linkage diagram of this type but are applied only to the specific case of resonant frequency tripling. The results revealed the presence of up to six Stark-shifted nonparametric resonances and the presence of saturation and interference effects on the parametric susceptibility. In particular, the third-order susceptibility is shown to saturate to a very small value under high-field conditions which restricts the range of useful pump intensities. Under near-resonant to resonant conditions, these imply that because of either nonparametric loss present at the pump or harmonic frequencies or power-dependent dispersive and saturation effects, conversion efficiencies higher than 25% may be difficult to realize in practice.

I. INTRODUCTION

Four-wave parametric interactions occur under a variety of experimental conditions and are used as a means of frequency generation or conversion and as a means of interrogating certain features of matter. It is well known that the nonlinear optical constants are frequency dependent and, as such, exhibit resonant enhancements which are exploited for certain applications.[1] For example, resonantly enhanced frequency tripling in phase-matched gases[2,3] and resonantly enhanced generation of tunable near-infrared radiation in gas-phase samples are but two common cases.[4-6]

For the most part, the usual resonant enhancement occurs with only one of the potentially many multiphoton resonances which are possible in a system, two-photon resonant being the most common. There are experimentally accessible situations for which all waves can be on resonance and for which one-, two-, and three-photon nonparametric effects exist under the same conditions as the parametric effect. Further complicating this situation is the potential for strong-field level shifts and splittings and simple population saturation. While adding great complexity to the understanding of resonant four-wave parametric interactions, a complete treatment of all these features is desirable in order to understand and evaluate the experiments and the potential utility of this type of interaction.

The earliest treatments of four-wave parametric interactions were based on a simple perturbative analysis[1] and perhaps modified to incorporate simple Stark effects.[7] There have been a few recent treatments of near-resonant four-wave interactions, most of which consider only partial resonance or some weak fields. Melikan and Saakyan and others investigated sub-T_2 pulse interactions in a frequency-tripling scenario for which optical nutation effects played a dominant role and found that, under cer-

tain conditions, full conversion of the pump into the third harmonic was possible.[8] This should be contrasted with the experimental behavior of two-photon resonant third-harmonic generation for which relatively low conversion efficiencies are found because of the presence of nonparametric effects.[2,3] Using as a basis the solutions for resonant three-wave interactions in a four-level system,[9] Tsukakoshi considered a perturbative fourth wave present under a nonperturbative pumping condition and showed, by direct calculations, some of the multitude of nonparametric resonances which may be present.[10] Expanding upon earlier treatments of tunable Raman emission in four-level systems,[5] Lin et al. studied the equivalent problem of two strong and two weak fields present in a four-wave parametric interaction and illustrated some Stark-shift effects.[11] Dick and Hochstrasser investigated the problem of resonant three- and four-wave interactions in three- and four-level systems and presented some results for the latter only in selected weak-field limits appropriate to CARS interactions.[12] Julien et al. have used the general results, to be presented here, to identify a naturally occurring four-wave parametric interaction in NH_3 involving only one input wave.[13] Most recently, Levine et al. have outlined a numerical diagonalization method for the resonant four-wave problem, in the limit where relaxation can be ignored, and illustrated some of the Stark multiplets which are present in such systems.[14] There have been other reports on this topic along with observations of fully resonant four-wave parametric interaction effects in molecular vapors, all of which suggest some interest and potential utility in this type of an effect.[15]

It is the purpose of this paper to present a general density-matrix formulation of resonant four-wave interactions in four-level systems appropriate to adiabatic pumping conditions. We make no restrictions on the relevant damping and dephasing parameters, so our re-

sults are valid for fully resonant conditions. Aside from documenting the analytical results, many for the first time, our main interest is in exploring this effect as a means of creating a large third-order nonlinearity for which the nonparametric losses are at a tolerable level. Our approach closely follows an earlier study on resonant three-wave parametric interactions in three-level systems, for which it was discovered that full conversion of the pump into the harmonic was possible under suitable conditions, so one goal of this paper is to ascertain if similar conditions exist for resonant frequency-tripling interactions.[16] Application of the results to other four-wave interaction cases will be presented elsewhere.[17]

In outline, the general equations are presented in Sec. II followed by a discussion of perturbative and strong-pump effects in Sec. III. Special emphasis is placed on the separate parametric and nonparametric interactions and the ac Stark-shifted multiplets. Explicit algebraic expressions are given for the multiplets and the parametric gain. These are followed by a summary and an Appendix which list the full algebraic solution for the coefficients of the nonlinear polarizations. Propagation issues are only briefly addressed in this paper.

II. BASIC EQUATIONS

The linkage diagram appropriate to near-resonant four-wave parametric interactions is shown in Fig. 1. Figure 1(a) is appropriate to resonant sum frequency or frequency tripling, 1(b) is appropriate to tunable stimulated Raman emission scenarios in the far infrared, and 1(c) is resonant CARS. Shown in Fig. 2 is an illustration of the number of the different processes associated with the ω_4 wave in Fig. 1(a) which can exist under resonant tuning conditions. It is clear from these diagrams and Fig. 1(a) that there is one one-wave interaction or transition 2(a), two two-wave interactions 2(b) and 2(c), three three-wave interactions 2(d)–2(f), and one four-wave interaction, all of which may be important simultaneously.

The familiar density matrix ρ for this system contains 16 terms, four population or diagonal elements and 12 off-diagonal elements. Using the electric-dipole approximation with nonzero transition dipole moments μ_{01}, μ_{12}, μ_{23}, and μ_{03}, the equations of motion for the off-diagonal elements appropriate to Fig. 1 are, from Schrödinger's equation $\dot{\rho} = [H, \rho]/i\hbar$,

$$\partial\rho_{01}/\partial t = -(i\Omega_{01} + 1/\tau_{01})\rho_{01} + [(\rho_{00} - \rho_{11})\mu_{01} \cdot \mathbf{E} + \rho_{02}\mu_{21} \cdot \mathbf{E} - \rho_{31}\mu_{03} \cdot \mathbf{E}]/i\hbar ,\tag{1}$$

$$\partial\rho_{12}/\partial t = -(i\Omega_{12} + 1/\tau_{12})\rho_{12} + [(\rho_{11} - \rho_{22})\mu_{12} \cdot \mathbf{E} + \rho_{13}\mu_{32} \cdot \mathbf{E} - \rho_{02}\mu_{10} \cdot \mathbf{E}]/i\hbar ,\tag{2}$$

$$\partial\rho_{23}/\partial t = -(i\Omega_{23} + 1/\tau_{23})\rho_{23} + [(\rho_{22} - \rho_{33})\mu_{23} \cdot \mathbf{E} + \rho_{20}\mu_{03} \cdot \mathbf{E} - \rho_{03}\mu_{20} \cdot \mathbf{E}]/i\hbar ,\tag{3}$$

$$\partial\rho_{03}/\partial t = -(i\Omega_{03} + 1/\tau_{03})\rho_{03} + [(\rho_{00} - \rho_{33})\mu_{03} \cdot \mathbf{E} + \rho_{02}\mu_{23} \cdot \mathbf{E} - \rho_{23}\mu_{02} \cdot \mathbf{E}]/i\hbar ,\tag{4}$$

$$\partial\rho_{02}/\partial t = -(i\Omega_{02} + 1/\tau_{02})\rho_{02} + [(\rho_{01}\mu_{12} \cdot \mathbf{E} + \rho_{03}\mu_{32} \cdot \mathbf{E} - \rho_{12}\mu_{01} \cdot \mathbf{E} - \rho_{32}\mu_{03} \cdot \mathbf{E})/i\hbar ,\tag{5}$$

$$\partial\rho_{13}/\partial t = -(i\Omega_{13} + 1/\tau_{13})\rho_{13} + [(\rho_{10}\mu_{03} \cdot \mathbf{E} + \rho_{12}\mu_{23} \cdot \mathbf{E} - \rho_{23}\mu_{12} \cdot \mathbf{E} - \rho_{03}\mu_{10} \cdot \mathbf{E})/i\hbar ,\tag{6}$$

where the phenomenological T_2 dephasing times are labeled as τ_{ij} and where the sign-dependent transition frequency is defined in terms of the eigenenergies E_i as $\Omega_{ij} = (E_i - E_j)/\hbar$ which have sign dependence.

Similarly, the equations of evolution for the diagonal elements are found to be

$$\partial\rho_{00}/\partial t = -(\rho_{00} - \rho_{00}^e)/\tau_{00} + [(\rho_{01} - \rho_{10})\mu_{10} \cdot \mathbf{E} + (\rho_{03} - \rho_{30})\mu_{30} \cdot \mathbf{E}]/\hbar ,\tag{7}$$

$$\partial\rho_{11}/\partial t = -(\rho_{11} - \rho_{11}^e)/\tau_{11} + [(\rho_{12} - \rho_{21})\mu_{21} \cdot \mathbf{E} + (\rho_{10} - \rho_{01})\mu_{01} \cdot \mathbf{E}]/\hbar ,\tag{8}$$

$$\partial\rho_{22}/\partial t = -(\rho_{22} - \rho_{22}^e)/\tau_{22} + [(\rho_{23} - \rho_{32})\mu_{32} \cdot \mathbf{E} + (\rho_{21} - \rho_{12})\mu_{12} \cdot \mathbf{E}]/\hbar ,\tag{9}$$

$$\partial\rho_{33}/\partial t = -(\rho_{33} - \rho_{33}^e)/\tau_{33} + [(\rho_{30} - \rho_{03})\mu_{03} \cdot \mathbf{E} + (\rho_{32} - \rho_{23})\mu_{23} \cdot \mathbf{E}]/\hbar ,\tag{10}$$

where the phenomenological T_1 decay times are labeled as τ_{ii} with equilibrium diagonal elements ρ_{ii}^e. The form of the T_1 terms is appropriate to bathlike situations in molecules and can be modified to include other kinetic relaxation situations such as those found in atomic cases. The specific form is not critical to our main results.

Next, we assume an optical-like interaction involving copropagating traveling waves by setting

$$\mathbf{E} = \sum_{i=1}^{4} \mathbf{E}_i \cos(\omega_i t - k_i z + \theta_i) ,$$

where θ_i are arbitrary phase factors and $\mathbf{E}_i$ are real, time-independent amplitudes with implied space dependence and polarization unit vector $\hat{\boldsymbol{\epsilon}}_i$. The latter is incor-
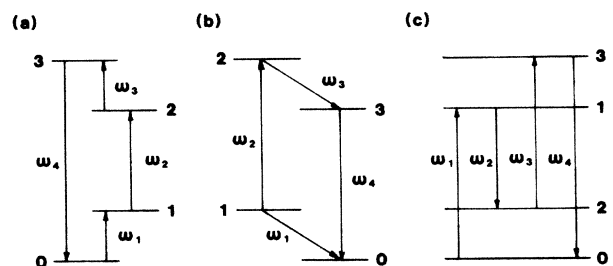
FIG. 1. Linkage diagram for four waves interacting in a four-level system forming a closed parametric loop. The different cases apply to (a) sum frequency generation and (b) tunable Raman emission when $\omega_2 = \omega_4$ and $\omega_1 = \omega_3$.
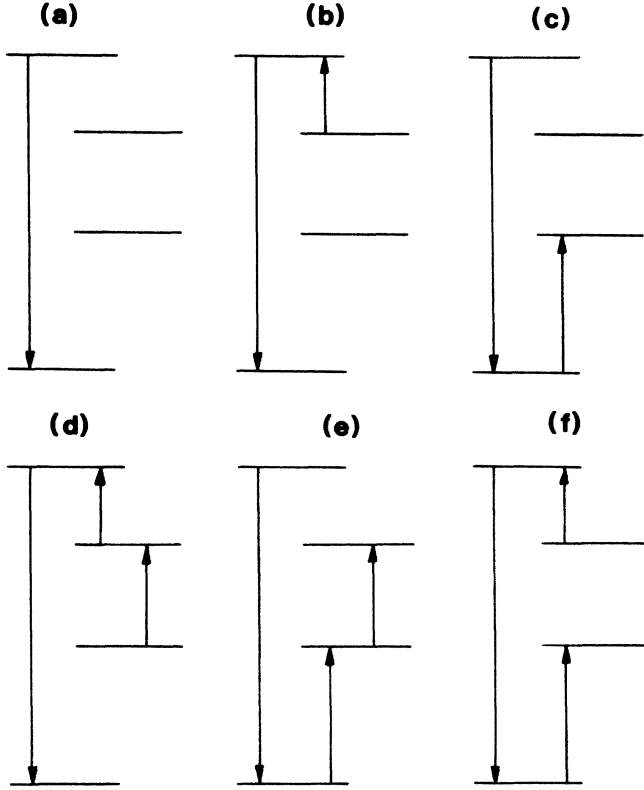
FIG. 2. Partial linkage diagrams appropriate to Fig. 1(a) showing separate multiphoton interactions involving the ω_4 wave; (a) one photon, (b) and (c) two photon, and (d), (e), and (f) three photon.

porated for generality so that level-degeneracy effects may be included via the m dependence of the matrix elements.[13,18]

Consistent with the near-resonant nature of the interaction, we assume that, for example, ω_1 is sufficiently close to Ω_{10} so that the dominant Fourier coefficients of ρ_{01} are at ω_1 and $\omega_4 - \omega_3 - \omega_2$. Using this observation and the rotating-wave approximation, the dominant Fourier contributions of ρ_{ij} can be identified as

$$\rho_{01} = \tilde{\rho}_{01}^{a} e^{i\omega_1 t} + \tilde{\rho}_{01}^{b} e^{i(\omega_4 - \sigma\omega_3 - \zeta\omega_2)t} , \tag{11}$$

$$\rho_{12} = \tilde{\rho}_{12}^{a} e^{i\zeta\omega_2 t} + \tilde{\rho}_{12}^{b} e^{i(\omega_4 - \omega_1 - \sigma\omega_3)t} , \tag{12}$$

$$\rho_{23} = \tilde{\rho}_{23}^{a} e^{i\sigma\omega_3 t} + \tilde{\rho}_{23}^{b} e^{i(\omega_4 - \omega_1 - \zeta\omega_2)t} , \tag{13}$$

$$\rho_{03} = \tilde{\rho}_{03}^{a} e^{i\omega_4 t} + \tilde{\rho}_{03}^{b} e^{i(\omega_1 + \zeta\omega_2 + \sigma\omega_3)t} , \tag{14}$$

$$\rho_{02} = \tilde{\rho}_{02}^{a} e^{i(\omega_1 + \zeta\omega_2)t} + \tilde{\rho}_{02}^{b} e^{i(\omega_4 - \sigma\omega_3)t} , \tag{15}$$

$$\rho_{13} = \tilde{\rho}_{13}^{a} e^{i(\zeta\omega_2 + \sigma\omega_3)t} + \tilde{\rho}_{13}^{b} e^{i(\omega_4 - \omega_1)t} , \tag{16}$$

where $\tilde{\rho}_{ij}^{q}$ are adiabatic constants to be determined, and $\sigma = +1$, $\zeta = +1$ for the linkage diagram shown in Fig. 1(a), $\sigma = -1$, $\zeta = +1$ for Fig. 1(b), and $\sigma = +1$, $\zeta = -1$ for Fig. 1(c). With these the most general reduction of Eqs. (11)–(16) occurs when $\omega_4 \neq \omega_1 + \zeta\omega_2 + \sigma\omega_3$. As an aside, any other linkage diagram may be treated in a straightforward manner by simply identifying the ap-

propriate Floquet coefficients of Eqs. (11)–(16) which ultimately appear in the definition of complex detunings.

Equations (1)–(6) are subsequently reduced to a set of algebraic equations by substituting into Eqs. (11)–(16), multiplying by the appropriate conjugate phase factors and using a short-time average to eliminate rapidly oscillating terms. The resulting algebraic equations, 24 in number, are expressed in terms of complex Rabi frequencies ($\Lambda_{ji} = \Lambda_{ij}^*$)

$$\Lambda_{01} = \mu_{01} \cdot E_1 e^{i\theta_1}/2\hbar, \quad \Lambda_{12} = \mu_{12} \cdot E_2 e^{i\zeta\theta_2}/2\hbar ,$$

$$\Lambda_{23} = \mu_{23} \cdot E_3 e^{i\sigma\theta_3}/2\hbar, \quad \Lambda_{03} = \mu_{03} \cdot E_4 e^{i\theta_4}/2\hbar$$

and complex detunings defined as

$$L_{01}^{a} = \Omega_{01} + \omega_1 - i/\tau_{01} ,$$

$$L_{12}^{a} = \Omega_{12} + \zeta\omega_2 - i/\tau_{12} ,$$

$$L_{23}^{a} = \Omega_{23} + \sigma\omega_3 - i/\tau_{23} ,$$

$$L_{03}^{a} = \Omega_{03} + \omega_4 - i/\tau_{03} ,$$

$$R_{02}^{a} = \Omega_{02} + \omega_1 + \zeta\omega_2 - i/\tau_{02} ,$$

$$R_{13}^{a} = \Omega_{13} + \zeta\omega_2 + \sigma\omega_3 - i/\tau_{13} ,$$

$$R_{02}^{b} = \Omega_{02} + \omega_4 - \sigma\omega_3 - i/\tau_{02} ,$$

$$R_{13}^{b} = \Omega_{13} + \omega_4 - \omega_1 - i/\tau_{13} ,$$

$$T_{01}^{b} = \Omega_{01} + \omega_4 - \sigma\omega_3 - \zeta\omega_2 - i/\tau_{01} ,$$

$$T_{12}^{b} = \Omega_{12} + \omega_4 - \sigma\omega_3 - \omega_1 - i/\tau_{12} ,$$

$$T_{23}^{b} = \Omega_{23} + \omega_4 - \zeta\omega_2 - \omega_1 - i/\tau_{23} ,$$

$$T_{03}^{b} = \Omega_{03} + \omega_1 + \zeta\omega_2 + \sigma\omega_3 - i/\tau_{03}$$

and are

$$T_{01}^{b} \tilde{\rho}_{01}^{b} = \Lambda_{03} \tilde{\rho}_{31}^{a} - \Lambda_{21} \tilde{\rho}_{02}^{b} , \tag{17}$$

$$T_{12}^{b} \tilde{\rho}_{12}^{b} = \Lambda_{10} \tilde{\rho}_{02}^{b} - \Lambda_{32} \tilde{\rho}_{13}^{b} , \tag{18}$$

$$T_{23}^{b} \tilde{\rho}_{23}^{b} = \Lambda_{21} \tilde{\rho}_{13}^{b} - \Lambda_{03} \tilde{\rho}_{20}^{a} , \tag{19}$$

$$T_{30}^{b} \tilde{\rho}_{30}^{b} = \Lambda_{32} \tilde{\rho}_{20}^{a} - \Lambda_{10} \tilde{\rho}_{31}^{a} , \tag{20}$$

$$R_{02}^{b} \tilde{\rho}_{02}^{b} = \Lambda_{01} \tilde{\rho}_{12}^{b} + \Lambda_{03} \tilde{\rho}_{32}^{a} - \Lambda_{12} \tilde{\rho}_{01}^{b} - \Lambda_{32} \tilde{\rho}_{03}^{a} , \tag{21}$$

$$R_{13}^{b} \tilde{\rho}_{13}^{b} = \Lambda_{10} \tilde{\rho}_{03}^{a} + \Lambda_{12} \tilde{\rho}_{23}^{b} - \Lambda_{23} \tilde{\rho}_{12}^{b} - \Lambda_{03} \tilde{\rho}_{10}^{a} , \tag{22}$$

$$R_{31}^{a} \tilde{\rho}_{31}^{a} = \Lambda_{30} \tilde{\rho}_{01}^{b} + \Lambda_{32} \tilde{\rho}_{21}^{a} - \Lambda_{01} \tilde{\rho}_{30}^{b} - \Lambda_{21} \tilde{\rho}_{32}^{a} , \tag{23}$$

$$R_{20}^{a} \tilde{\rho}_{20}^{a} = \Lambda_{21} \tilde{\rho}_{10}^{a} + \Lambda_{23} \tilde{\rho}_{30}^{b} - \Lambda_{10} \tilde{\rho}_{21}^{a} - \Lambda_{30} \tilde{\rho}_{23}^{b} , \tag{24}$$

$$L_{10}^{a} \tilde{\rho}_{10}^{a} = \Lambda_{10}(\rho_{00} - \rho_{11}) + \Lambda_{12} \tilde{\rho}_{20}^{a} - \Lambda_{30} \tilde{\rho}_{13}^{b} , \tag{25}$$

$$L_{21}^{a} \tilde{\rho}_{21}^{a} = \Lambda_{21}(\rho_{11} - \rho_{22}) + \Lambda_{23} \tilde{\rho}_{31}^{a} - \Lambda_{01} \tilde{\rho}_{20}^{a} , \tag{26}$$

$$L_{32}^{a} \tilde{\rho}_{32}^{a} = \Lambda_{32}(\rho_{22} - \rho_{33}) + \Lambda_{30} \tilde{\rho}_{02}^{b} - \Lambda_{12} \tilde{\rho}_{31}^{a} , \tag{27}$$

$$L_{03}^{a} \tilde{\rho}_{03}^{a} = -\Lambda_{03}(\rho_{00} - \rho_{33}) - \Lambda_{23} \tilde{\rho}_{02}^{b} + \Lambda_{01} \tilde{\rho}_{13}^{b} . \tag{28}$$

The remaining 12 equations are the complex conjugate of these. For these, the complex detuning is defined as the negative of the conjugate detuning (L, R or $T)_{ji}^{a \text{ or } b} = -[(L, R \text{ or } T)_{ij}^{a \text{ or } b}]^*$.

The interrelationship between the various diagonal and

off-diagonal terms is shown in the signal flow graph of Fig. 3 which is a picture of Eqs. (17)–(28) and the conjugate equations and is discussed more fully elsewhere.[19] The nodes in the graph represent the time-independent Floquet coefficients of the off-diagonal elements and the diagonal elements, which are independent variables in these equations. The arrows point from the appropriate node on the right-hand side of Eqs. (17)–(28) to the node, or element in question and the label above the arrow is the Rabi frequency multiplier in the equations. The shorthand notation for the Rabi frequencies is that A, B, C, and D are Λ_{01}, Λ_{12}, Λ_{23}, and Λ_{03}, respectively, for the solid arrows and the conjugate of these for the open arrows. The main utility of the graph is in the ease with which the interrelationships between elements can be visualized and in determining perturbative and nonperturbative solutions using a powerful graph algebra, which is fully equivalent to Cramer's rule. Since the graph is a picture of the original equations, it should not be confused with other graph approaches which are pictures of

one order of an interaction.[20]

The obvious grouping of the equations into two decoupled sets of 12 equations occurs because of the dissection of the individual off-diagonal elements into parametric and nonparametric terms in Eqs. (11)–(16). While clearly doubling the number of equations which must be treated, this decomposition ultimately leads to a full separation of the two different kinds of processes which might be present, thus permitting a separate consideration of each. The solution of the set of equations, in which population differences appear as independent variables, is listed in the Appendix.

The next step in the calculation entails the determination of the individual population values under the influence of the fields. Using Eqs. (11)–(16) and a short-time average, the four driving terms in the equations of motion (1)–(6) become

$$\rho_{01}\mu_{10}\cdot\mathbf{E}/\hbar \longrightarrow \tilde{\rho}_{01}^{a}\Lambda_{10}+\tilde{\rho}_{01}^{b}\Lambda_{10}F \ , \tag{29}$$

$$\rho_{12}\mu_{21}\cdot\mathbf{E}/\hbar \longrightarrow \tilde{\rho}_{12}^{a}\Lambda_{21}+\tilde{\rho}_{12}^{b}\Lambda_{21}F \ , \tag{30}$$

$$\rho_{23}\mu_{32}\cdot\mathbf{E}/\hbar \longrightarrow \tilde{\rho}_{23}^{a}\Lambda_{32}+\tilde{\rho}_{23}^{b}\Lambda_{32}F \ , \tag{31}$$

$$\rho_{03}\mu_{30}\cdot\mathbf{E}/\hbar \longrightarrow \tilde{\rho}_{03}^{a}\Lambda_{30}+\tilde{\rho}_{03}^{b}\Lambda_{30}F^{*} \ , \tag{32}$$

where a phase factor has been defined as

$$F=\exp[i(\omega_{4}-\sigma\omega_{3}-\zeta\omega_{2}-\omega_{1})t$$
$$-i(k_{4}-\sigma k_{3}-\zeta k_{2}-k_{1})z] \ . \tag{33}$$

The factor F clearly labels the parametric terms in Eqs. (29)–(32) and simply expresses the familiar degradation of the interaction if conservation of energy and momentum are both not satisfied between the interacting waves. For purposes of graphical displays, F will be replaced by a real Lorentzian centered at the four-wave parametric resonant frequency of $\omega_{4}=\sigma\omega_{3}+\zeta\omega_{2}+\omega_{1}$.

The solution of Eqs. (7)–(10), which are performed numerically, are then used to determine the specific value of the off-diagonal elements under the influence of the fields at some space point. The macroscopic polarization is found from $\mathbf{P}=N\,\mathrm{Tr}(\rho\mu)$, where N is the number density of four-level systems. Since $\mathbf{P}$ is real as defined, the equivalent complex macroscopic polarizations are $\mathbf{P}_{1}=N\mu_{10}\rho_{01}$, $\mathbf{P}_{2}=N\mu_{21}\rho_{12}$, $\mathbf{P}_{3}=N\mu_{32}\rho_{23}$, and $\mathbf{P}_{4}=N\mu_{30}\rho_{03}$, where ρ_{ij} are given by Eqs. (12)–(16). These polarizations can be used to formally define a Beer's coefficient, for nonparametric terms, or a conversion distance, for parametric terms, or used as source terms in numerical simulations of propagation effects as illustrated elsewhere.[16] The multiphoton nature of the interaction in terms of saturation and level splittings, and their effect on the separate parametric and nonparametric polarizations will be now illustrated.
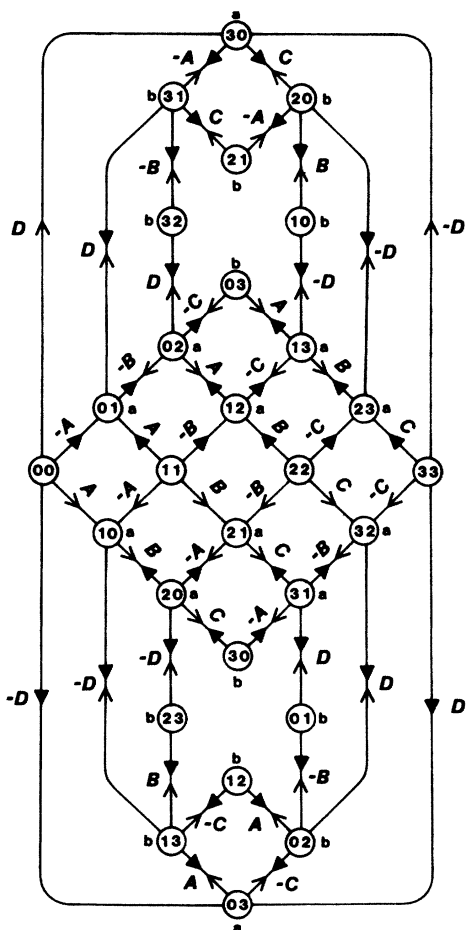
FIG. 3. Signal flow graph representation of the original density-matrix equations when reduced to a set of coupled algebraic equations. The nodes refer to the diagonal and off-diagonal Floquet elements. The lines are labeled with the Rabi frequencies appearing as multipliers in the equations where the solid and open arrow refers to the Rabi frequency or its conjugate.

III. LOCAL SOLUTIONS

A. Perturbation limit

Although the formalism presented so far is applicable to harmonic generation, sum and difference frequency generation, and CARS, we specialize at this point to the

specific case of third-harmonic generation by setting $\omega_1=\omega_2=\omega_3$, $E_1=E_2=E_3$, $k_1=k_2=k_3$, $\theta_1=\theta_2=\theta_3=0$, and $\sigma=\zeta=+1$. The relevant macroscopic polarization driving the harmonic is

$$P_4=N\mu_{30}(\tilde{\rho}^{\,a}_{03}e^{i\omega_4 t}+\tilde{\rho}^{\,b}_{03}e^{i3\omega_1 t}) \tag{34}$$

and is clearly separated into nonparametric, $\tilde{\rho}^{\,a}_{03}$, and parametric, $\tilde{\rho}^{\,b}_{03}$, terms.

The perturbation limit, which arises when all waves are weak, may be extracted from the results in the Appendix or directly from the signal flow graph.[19] The lowest-order contribution to the nonparametric element, $\tilde{\rho}^{\,a}_{03}$, is simply

$$\tilde{\rho}^{\,a}_{03}=\frac{\Lambda_{03}(\rho_{33}-\rho_{00})}{L^a_{03}} \ , \tag{35}$$

which is the one-photon absorption term since it is maximum when $\omega_4=\Omega_{30}$.

For the parametric term $\tilde{\rho}^{\,b}_{03}$ the perturbation solution is

$$\tilde{\rho}^{\,b}_{03}=\frac{\Lambda_{01}\Lambda_{12}\Lambda_{23}}{T^b_{03}}\left[\frac{\rho_{11}-\rho_{00}}{R^a_{02}L^a_{01}}\right.$$
$$-\left[\frac{1}{R^a_{02}}+\frac{1}{R^a_{13}}\right]\frac{\rho_{22}-\rho_{11}}{L^a_{12}}$$
$$\left.+\frac{\rho_{33}-\rho_{22}}{R^a_{13}L^a_{23}}\right] \ . \tag{36}$$

The presence of the complex detunings reveals the conditions for resonant enhancement. One such resonant enhancement occurs, from T^b_{03}, when the pump is at least on three-photon resonance, $\Omega_{30}=3\omega_1$. If $\rho_{00}=\rho^e_{00}=1$, a second resonance enhancement occurs, from R^a_{02}, when the pump is on two-photon resonance, $\Omega_{20}=2\omega_1$, and a third resonance enhancement is associated with L^a_{01} when the pump is on one-photon resonance, $\Omega_{10}=\omega_1$. If $\rho_{00}=\rho^e_{00}\neq 1$, then the three terms in the large square brackets may interfere causing a local minimum in the nonlinear susceptibility with pump detuning. If $\rho_{00}=\rho^e_{00}=1$ and the pump is on one- two-, and three-photon resonance, the parametric term approaches a maximum value of

$$\rho^b_{03}\rightarrow i\tau_{01}\tau_{02}\tau_{03}\Lambda_{01}\Lambda_{12}\Lambda_{23}\propto |E_1|^3 \ .$$

However, under these conditions, the harmonic and the pump are experiencing large nonparametric losses which can only be partially suppressed by increasing the pump

field. In the strong-pump regime, this simple cubic scaling of ρ^b_{03} and the nonparametric losses are both modified because of population saturation and ac Stark shifts as will be illustrated shortly.

In the case of resonant second-harmonic generation for which a harmonic was tuned near Ω_{20} in Fig. 1, it was found that if $\mu_{12}\gg\mu_{01}$, the dominant pump ac Stark effect was such that the Ω_{10} and Ω_{20} transitions were split into doublets such that the material was essentially transparent to the pump and harmonic, but that under the same conditions the parametric gain saturated to a very large value.[16] The obvious question is to ask if similar circumstances can occur in this case. If so, then the fully resonant case is a candidate scenario for efficient frequency tripling.

B. Strong-pump limit

The strong-pump and harmonic limits are contained in the solutions listed in the Appendix. Of special interest is the case of a weak harmonic, which might be thought of as a probe of the optical properties of the system. Even in this limit, the results are quite complex because of population saturation and strong-field level shifts so only a limited amount of analytical manipulations are feasible here.

As an aid in understanding the nonparametric spectra, the location of the resonances can be determined by the following method. Each off-diagonal element is linearly dependent on the diagonal elements, which in turn are nonlinearly dependent on the fields. Because of this linear dependence, the superposition principle may be used in reverse to simplify the expressions for the off-diagonal elements ultimately yielding simplified results for the spectra. To implement this, we choose the synthetic condition obtained by setting $\rho_{00}=1$. The nonparametric solution for this case will describe all transitions associated with level $|0\rangle$ and will contain ac Stark information but will not, clearly, yield the correct saturated Beer's coefficient.[21] The utility of this limit rests with the ease with which the Stark-shifted resonances may be determined.

In the limit $\Lambda_{03}\rightarrow 0$ and $\rho_{00}\rightarrow 1$, the nonparametric part of the off-diagonal element, $\tilde{\rho}^{\,a}_{03}$, responsible for the optical properties sensed by the harmonic becomes

$$\tilde{\rho}^{\,a}_{03}\,|_{\Lambda_{03}\rightarrow 0}=\frac{-\Lambda_{30}\rho_{00}\delta_1}{L^a_{03}\Delta_1}=\frac{-\Lambda_{03}\rho_{00}}{L_{net}} \ , \tag{37}$$

where, setting $\Lambda^2_{ij}=\Lambda_{ij}\Lambda_{ji}=\Lambda_{ij}\Lambda^*_{ij}$,

$$\Delta_1=1-\frac{\Lambda^2_{01}}{L^a_{03}R^b_{13}}-\frac{\Lambda^2_{01}}{R^b_{02}T^b_{12}}-\frac{\Lambda^2_{12}}{R^b_{13}T^b_{23}}-\frac{\Lambda^2_{12}}{R^b_{02}T^b_{01}}-\frac{\Lambda^2_{23}}{L^a_{03}R^b_{02}}-\frac{\Lambda^2_{23}}{R^b_{13}T^b_{12}}-\frac{2\Lambda^2_{01}\Lambda^2_{23}}{L^a_{03}R^b_{02}R^b_{13}T^b_{12}}$$
$$+\frac{\Lambda^2_{01}\Lambda^2_{12}}{R^b_{02}R^b_{13}T^b_{12}T^b_{23}}+\frac{\Lambda^4_{12}}{R^b_{02}R^b_{13}T^b_{01}T^b_{23}}+\frac{\Lambda^2_{12}\Lambda^2_{23}}{L^a_{03}R^b_{02}R^b_{13}T^b_{23}}+\frac{\Lambda^4_{01}}{L^a_{03}R^b_{02}R^b_{13}T^b_{12}}$$
$$+\frac{\Lambda^2_{01}\Lambda^2_{12}}{L^a_{03}R^b_{02}R^b_{13}T^b_{01}}+\frac{\Lambda^2_{12}\Lambda^2_{23}}{R^b_{02}R^b_{13}T^b_{01}T^b_{12}}+\frac{\Lambda^4_{23}}{L^a_{03}R^b_{13}R^b_{02}T^b_{12}}$$

FIG. 4. Graphs for the optical properties of the system sensed by the ω_4 wave in Fig. 1(a). The curves labeled abs and disp refer to the imaginary and real parts of the nonparametric off-diagonal element $\tilde{\rho}_{03}^a/\Lambda_{03}$ and control the absorption and refractive index. The lower curve shows just the bare cross section, $\mathrm{Im}(L_{\mathrm{net}}^{-1})$, and the ticks show the resonances determined from Eq. (38). The last curve shows the third-harmonic parametric amplitude $|\tilde{\rho}_{03}^b|$ and two possible second-harmonic amplitudes (02 and 13). The ω_4 detuning is in units of $(\Omega_{30}-\omega_4)T_2$. The upper and lower group of numbers in each figure refer to the pump conditions: $\Lambda_{01}T_2$, $\Lambda_{12}T_2$, $\Lambda_{23}T_2$, and $(\Omega_{10}-\omega_1)T_2$, $(\Omega_{21}-\omega_2)T_2$, $(\Omega_{32}-\omega_3)T_2$.

and where δ_1 is Δ_1 with L_{03}^a replaced by ∞. The total expression can be recast into some generalized complex detuning function L_{net} with implied Stark shifts.[21,22] By definition, resonances are associated with those values of frequency ω_4 for which the denominator becomes purely complex. From the practical point of view, the Stark multiplet is only resolvable if the splittings are greater than a linewidth. Anticipating this, L_{net} can be simplified in the sharp-line limit by setting the i/τ_{ij} terms to zero yielding what might be called a root equation

$$W(Z-W)(X-W)(Y+Z-W)(X+Z-W)(X+Y-W)$$

$$= \Lambda_{12}^2 W(X+Z-W)[(X-W)(X+Y-W)+(Z-W)(Y+Z-W)]$$

$$+ \Lambda_{01}^2 \Lambda_{12}^2 [(X+Z-W)(X+Y-W)-W(Y+Z-W)]+(Y+Z-W)(X+Y-W)(\Lambda_{01}^2-\Lambda_{23}^2)^2$$

$$- \Lambda_{01}^2 (Y+Z-W)(X+Y-W)[(Z-W)(X+Z-W)-W(X-W)]-\Lambda_{12}^4 W(X+Z-W)$$

$$- \Lambda_{23}^2 (Y+Z-W)(X+Y-W)[(X-W)(X+Z-W)-W(Z-W)]$$

$$+ \Lambda_{12}^2 \Lambda_{23}^2 [(Y+Z-W)(X+Z-W)-W(X+Y-W)] , \tag{38}$$

where $X=(\Omega_{10}-\omega_1)$, $Y=(\Omega_{21}-\omega_2)$, $Z=(\Omega_{32}-\omega_3)$, and $W=(\Omega_{30}-\omega_4)$. The detunings on the left-hand side of this equation, which specify the zero-field resonances, show that in the most general case, the equation is of sixth order in W and thus leads to at most six resonances, one for each nonparametric resonance seen in Fig. 2.[23] These resonances are fully equivalent to the allowed transitions between the dressed states of the system, and the strength of each may be found from Eq. (37), namely from $\text{Im}(L_{net}^{-1})$.[21] As an example, if the pump is on full resonance, the roots are simple to obtain and are

$$\Omega_{30}-\omega_4=0, \pm\{[(\Lambda_{01}\pm\Lambda_{23})^2+\Lambda_{12}^2]\}^{1/2} .$$

Thus at full resonance, the $|0\rangle \rightarrow |3\rangle$ transition may be split into a quintet with a possible loss on parametric resonance, $\Omega_{30}-\omega_4=0$.

Under the same strong-pump, but weak-probe, conditions, the parametric contribution is found to be[22]

$$\tilde{\rho}_{03}^b = \frac{\Lambda_{01}\Lambda_{12}\Lambda_{23}}{T_{03}^b \Delta_2} \left\{ \frac{\rho_{11}-\rho_{00}}{L_{01}^a R_{02}^a} \left[1 + \frac{\Lambda_{01}^2-\Lambda_{23}^2}{L_{12}^a R_{13}^a} - \frac{\Lambda_{12}^2}{L_{23}^a R_{13}^a} \right] \right.$$

$$- \frac{\rho_{22}-\rho_{11}}{L_{12}^a} \left[\frac{1}{R_{02}^a} \left(1 - \frac{\Lambda_{12}^2}{L_{23}^a R_{13}^a} \right) + \frac{1}{R_{13}^a} \left(1 - \frac{\Lambda_{12}^2}{L_{01}^a R_{02}^a} \right) \right]$$

$$\left. + \frac{\rho_{33}-\rho_{22}}{L_{23}^a R_{13}^a} \left[1 + \frac{\Lambda_{23}^2-\Lambda_{01}^2}{L_{12}^a R_{02}^a} - \frac{\Lambda_{12}^2}{L_{01}^a R_{02}^2} \right] \right\} , \tag{39}$$

where

$$\Delta_2 = 1 - \frac{\Lambda_{01}^2}{L_{12}^a R_{02}^a} - \frac{\Lambda_{01}^2}{R_{13}^a T_{03}^b} - \frac{\Lambda_{12}^2}{L_{01}^a R_{02}^a} - \frac{\Lambda_{12}^2}{L_{23}^a R_{13}^a} - \frac{\Lambda_{23}^2}{R_{02}^a T_{03}^b} - \frac{\Lambda_{23}^2}{L_{12}^a R_{13}^a} - \frac{2\Lambda_{01}^2\Lambda_{23}^2}{L_{12}^a R_{02}^a R_{13}^a T_{03}^b}$$

$$+ \frac{\Lambda_{01}^2\Lambda_{12}^2}{L_{01}^a R_{02}^a R_{13}^a T_{03}^b} + \frac{\Lambda_{12}^4}{L_{01}^a R_{02}^a L_{23}^a R_{13}^a} + \frac{\Lambda_{12}^2\Lambda_{23}^2}{L_{01}^a R_{02}^a L_{12}^a R_{13}^a} + \frac{\Lambda_{01}^4}{L_{12}^a R_{02}^a R_{13}^a T_{03}^b}$$

$$+ \frac{\Lambda_{01}^2\Lambda_{12}^2}{L_{12}^a R_{02}^a L_{23}^a R_{13}^a} + \frac{\Lambda_{12}^2\Lambda_{23}^2}{L_{23}^a R_{13}^a R_{02}^a T_{03}^b} + \frac{\Lambda_{23}^4}{L_{12}^a R_{13}^a R_{02}^a T_{03}^b} . \tag{40}$$

Since the detunings in Eq. (40) are independent of ω_4 then from the factor F, $\tilde{\rho}_{03}^b$ has an implied parametric resonance when $\omega_4=\omega_1+\omega_2+\omega_3=3\omega_1$. The complex term Δ_2 scales as $\mathscr{E}^4$ so that each diagonal element has a multiplier which scales as $\mathscr{E}^5/\mathscr{E}^4$ or $\mathscr{E}$. Considering simple saturation only, the diagonal element difference is expected to scale as $1/\mathscr{E}^2$ so that $\tilde{\rho}_{03}^b$ is expected to scale as $1/\mathscr{E}$ in the strong-field limit. This feature is in marked contrast with the resonant second-harmonic generation case for which the strong-pump parametric term approached a constant. As a particular example, if the pump is on full resonance and for roughly equal matrix elements

$\Lambda_{01}\approx\Lambda_{12}\approx\Lambda_{23}=\Lambda$ and $\tau_{ij}=\tau_{ii}=T_2$, the parametric term can be evaluated in closed form as

$$\tilde{\rho}_{03}^b = \frac{i}{30\Lambda T_2} [\rho_{00}^e-\rho_{33}^e+3(\rho_{22}^e-\rho_{11}^e)] \rightarrow 0 \tag{41}$$

which shows that under fully saturated, strong-field conditions, the parametric contribution becomes vanishingly small, showing that any nonparametric losses present cannot be arbitrarily overcome simply with larger pumping fields.

Figure 4 shows a family of plots of the spectral properties of the material under strong-pumping but weak-

probing conditions. For these examples we have chosen $\tau_{ij} = \tau_{ii} = T_2$ and $\rho_{00}^e = 1$. All frequency terms are expressed in units of T_2 so that the ω_4 detuning in these figures is $(\Omega_{30} - \omega_4)T_2 = WT_2$ and the strong-field Rabi frequencies are expressed as ΛT_2 so that $(\Lambda T_2)^2 = I/I_{sat}$, where I_{sat} is the conventional saturation intensity of a transition. The lower curve in Fig. 4 is $\mathrm{Im}(L_{net}^{-1})$ from Eq. (37) with a norm of unity and the ticks under this curve show the resonances determined from Eq. (38); however, only the optically active ones are shown for clarity. The upper group of curves are as follows. The real and imaginary parts of $-\tilde{\rho}_{03}^a/\Lambda_{03}$, with contributions from all states, control the dispersion (disp) and absorption (abs) at ω_4 and are shown because of their importance in phasing matching and attenuation. The absolute value of three parametric terms (para) are displayed, $\tilde{\rho}_{03}^b$, $\tilde{\rho}_{02}^a$, and $\tilde{\rho}_{13}^a$, and reflect the third-harmonic and two possible second-harmonic polarizations.[16,24] The latter two are displayed shifted from the third-harmonic polarization by -10 and $+10$ detuning units, respectively. The upper group of numbers shown in the figure refer to the pump wave Rabi frequencies in the order $\Lambda_{01}T_2$, $\Lambda_{12}T_2$ and $\Lambda_{23}T_2$, and the lower group of numbers refer to the respective detunings in the order $(\Omega_{10} - \omega_1)T_2 = XT_2$, $(\Omega_{21} - \omega_2)T_2 = YT_2$, and $(\Omega_{32} - \omega_2)T_2 = ZT_2$.

Figure 4(a) is for the case of a fully resonant pump with approximately equal matrix elements. As seen in this figure, the third-harmonic parametric gain is almost zero in accord with the implications of Eq. (41) leaving only the possibility of a second-harmonic gain and a small nonparametric gain near detunings of ± 8. The resonances predicted by Eq. (38) are in excellent agreement with direct calculations.

Figures 4(b) and 4(c) are also appropriate to a fully resonant pumping situation but with different matrix elements. For Fig. 4(b), μ_{12} is set to be 5 times higher than $\mu_{01} = \mu_{23}$, while for Fig. 4(c), μ_{23} is set to be 5 times higher. For these, the strongest Rabi frequency should dominate the Stark multiplet. For the conditions of Fig. 4(c), the ω_3 wave should split the Ω_{32} transition into a doublet which should result in a reduction of losses at the harmonic, as seen, but also results in a very small parametric gain because of the interference effects from the highly populated excited states. For the conditions of Fig. 4(b), the ω_2 wave should split the Ω_{21} transition into a doublet which should result in reduced pump absorption and hence a minimum value of saturation. This is indeed the case as evident by the large parametric gain but also a very large nonparametric loss.

Figures 4(a), 4(d), and 4(e) show a sequence of results when the pump is on three- $(\Omega_{30} = \omega_1 + \omega_2 + \omega_3)$ and two- $(\Omega_{20} = \omega_1 + \omega_2)$ photon resonance as the one-photon detuning, $(\Omega_{10} - \omega_1)T_2 = -(\Omega_{21} - \omega_2)T_2$, is varied. As seen in this sequence, the dispersion at parametric resonance is small, the parametric amplitude increases somewhat with detuning because of reduced saturation but there is some nonparametric loss. In the far-wing limit of the detuning, $(\Omega_{10} - \omega_1)T_2 < -100$, there is little saturation and the Stark shifts are dominated by ω_3 such that Ω_{32} is split

into a doublet, thus splitting the nonparametric resonance Ω_{30} into a doublet, reducing the loss on parametric resonance. However, because the pump is in the wing of the main absorption line, there is an implied power dependence to the pump dispersion. The scaling of the parametric polarization in this limit is most unusual, approaching

$$\tilde{\rho}_{03}^b = -\frac{\Lambda_{01}\Lambda_{12}\Lambda_{23}\tau_{02}\tau_{03}\rho_{00}}{(\Omega_{01} + \omega_1)(1 + \Lambda_{23}^2\tau_{03}\tau_{02})} \propto \mathscr{E}_1 , \qquad (42)$$

which was verified by direct simulation. This result is a direct consequence of ac Stark degradation caused by the resonant ω_3 wave.

Figures 4(f) and 4(g) show the results of a permutation of the detuning conditions of Fig. 4(e). For Fig. 4(g), because of the detunings, saturation is slight resulting in a very large loss on parametric resonance. For Fig. 4(f), because the ω_1 wave is on resonance, the lowest two states are highly saturated resulting in a reduced parametric gain and nonparametric loss. The far-wing limit of this case is very similar to the results in Eq. (42), but half the magnitude because of saturation. It is also of interest to note that the second-harmonic polarization is not negligible in this case and reflects only one of the detuning combinations explored experimentally by Yngvesson and Kollberg, for which efficient doubling was obtained.[25]

Figure 4(h) shows the results for a detuning condition for which the pump is only on triple resonance. For this case, there is a significant parametric gain but also nonparametric loss and dispersion.

C. Implications

The results displayed in Fig. 4, while not exhaustive in terms of ranges in the variables, strongly suggest that it will be difficult to realize efficient, $\approx 100\%$, frequency tripling in general in this type of interaction. This conclusion follows from Fig. 4 in which are shown conditions for which there is either a strong nonparametric loss present at the harmonic or pump frequencies, or both, or dispersion at the harmonic frequency with an implied power-dependent phase-match condition.

Some computer simulations of a propagation model of the frequency-tripling interaction were explored for conditions similar to those in Fig. 4. The spatial growth of the waves is governed by[16]

$$\partial\Lambda_{01}/\partial\xi = \mathrm{Re}[-i(\tilde{\rho}_{01}^a + \tilde{\rho}_{01}^b F) - iR_b(\tilde{\rho}_{12}^a + \tilde{\rho}_{12}^b F)$$
$$-iR_c(\tilde{\rho}_{23}^a + \tilde{\rho}_{23}^b F)] ,$$

$$\partial|\Lambda_{03}|/\partial\xi = \frac{k_4}{k_1}R_a\mathrm{Re}[-i(\tilde{\rho}_{03}^a + \tilde{\rho}_{03}^b F)e^{-i\theta_4}] ,$$

where F is given in Eq. (33),

$$R_b = \mu_{23}\cdot\hat{\epsilon}_1/\mu_{10}\cdot\hat{\epsilon}_1, \quad R_c = \mu_{32}\cdot\hat{\epsilon}_1/\mu_{10}\cdot\hat{\epsilon}_1 ,$$

and

$$R_a = |\mu_{30}\cdot\hat{\epsilon}_4|^2/|\mu_{10}\cdot\hat{\epsilon}_1|^2 .$$

The normalized spatial variable ξ is $Nk_1 |\mu_{10}\cdot\hat{\epsilon}_1|^2 z/2\hbar\epsilon$,
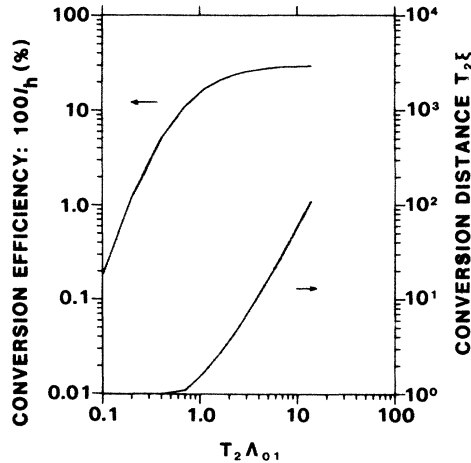
FIG. 5. Numerical simulation of the coupled wave equations for the pump and third harmonic for full resonance, $\rho_{00}^e = 1$, and matrix elements in the ratio $\mu_{21} \cdot \hat{\epsilon}_1 / \mu_{10} \cdot \hat{\epsilon}_1 = 4$, $\mu_{32} \cdot \hat{\epsilon}_1 / \mu_{10} \cdot \hat{\epsilon}_1 = 3$, $\mu_{30} \cdot \hat{\epsilon}_4 / \mu_{10} \cdot \hat{\epsilon}_1 = 1$, $\tau_{ii} = \tau_{ij} = T_2$, and perfect phase matching is assumed throughout the interaction length. The conversion efficiency, $I_h = |E_4(\xi)|^2 / |E_1(0)|^2$, has a maximum value for the indicated conversion distance, $T_2\xi$. For distances beyond these, both waves are attenuated further.

where N is the number density of entities and z is the real-space variable. For reference purposes, $T_2\xi = \alpha z$, where α is the unsaturated *field* Beer's coefficient at line center.

Under fully resonant conditions, there will be no power-dependent dispersion caused by saturation or Stark shifts of the transitions under consideration. These equations can then be solved numerically by assuming a perfect phase-matched condition by replacing F by a narrow Lorentzian. Figure 5 shows the results of one such set of simulations for the conversion efficiency and conversion distance for a near-optimized choice of matrix elements. The saturation of the efficiency at a value of 24% rather than 100% is due exclusively to the saturated absorption present under these resonant conditions.

Figure 6 illustrates the far-wing limit of the case shown in Fig. 4(e) both with[17] and without the power-dependent dispersion. As seen in these results, the power-dependent dispersion has a predictably major effect on the overall conversion efficiency, degrading it by a factor of 10. Interestingly, pump-induced dispersive effects were also found to dominate two-photon resonant frequency-tripling interactions[3] and are thought to be present in other four-wave systems.[13]

IV. CONCLUSIONS

In summary, we have presented general analytical results for the nonlinear optical polarization appropriate to the case of resonant four-wave interactions in a four-level system in the adiabatic limit. The results were applied to the specific case of frequency tripling with a goal of assessing this interaction for efficient conversion. The most important analytical results are expressed in Eqs. (37)–(40). Regarding frequency tripling, under near to

resonant conditions, either nonparametric loss or power-dependent dispersive effects are present and act as ultimate limits to efficient conversion, restricting the latter to a maximum of about 25% under conditions which would be difficult to realize experimentally. It remains to be determined if similar limitations exist for some of the other pump-emission combinations shown in Fig. 1, particularly those dominated by a four-wave parametric gain.

The solutions presented in this paper complete the simplest treatment of multiple-wave interactions in four-level systems which were arrived at by assuming adiabatic conditions and monochromatic fields. The other two combinations involve either a serial three-wave interaction,[9] such as a three-photon absorption, or a parallel three-wave interaction,[26] such as a second, competing Raman wave, and are easily understood using the same techniques outlined in this paper.

Because of the distinct possibility of transcription errors in the equations, interested readers may obtain either a printed listing of the computer programs used in this
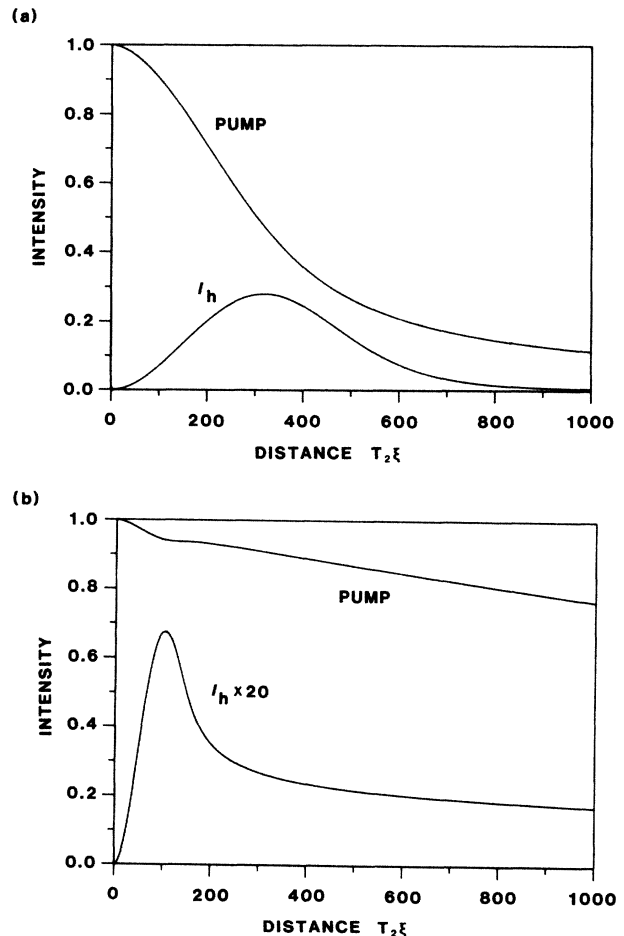
FIG. 6. Numerical simulation of the evolution of the pump and third harmonic for (a) perfect phase matching and (b) power-dependent phase matching. The conditions are similar to Fig. 4(e) and Fig. 5 except for the following: $\mu_{21} \cdot \hat{\epsilon}_1 / \mu_{10} \cdot \hat{\epsilon}_1 = 1$, $\mu_{32} \cdot \hat{\epsilon}_1 / \mu_{10} \cdot \hat{\epsilon}_1 = 10$, $(\Omega_{10} - \omega_1)T_2 = 100$, $(\Omega_{21} - \omega_2)T_2 = -100$, and $\Lambda_{01}T_2 = 4$. Distance is in units of $T_2\xi$, and the intensities are defined by $I_k = |E_k(\xi)|^2 / |E_1(0)|^2$, where k is the pump or harmonic label.

study or a copy on a floppy disk (IBM 360k format) by direct request from the first author (T.A.D.).

Note added. The dressed-atom approach has recently been used by Wang, Wang, and Fu[27] to study the case of Fig. 1(b) when only two of the waves are strong as in Ref. 11. Further, Tai, Deck, and Kim[28] have recently presented more data on frequency summation, $2\omega_1 + \omega_3$, in four-level system in I_2 and considered Stark effects on the nonlinear polarization in the wing limit of the detunings.

ACKNOWLEDGMENTS

APPENDIX

The full solution of Eqs. (17)–(28) is achieved by treating the diagonal elements as independent variables, expressing the off-diagonal elements in terms of these and various coefficients, and then solving Eqs. (7)–(10) for the actual value of the diagonal elements. The true diagonal elements are thus found and may be used as source terms in Maxwell's equations for example. The most complex part of this is in the first step. Interestingly, algebraic equivalents of FORTRAN are of no use since they invariably yield a result in the form of some polynomial which is not necessarily the most compact form nor even readable in some cases. For combinatorial problems such as this one, a compact result often takes the form of a continued fraction, and the results below are in fact combinations of nested continued fractions.

Each off-diagonal element will be expressed in terms of coefficients which are multipliers to the four possible diagonal-element differences associated with the four possible one-photon transitions. Thus, for example, the two off-diagonal amplitudes in Eq. (14) become

$$\tilde{\rho}_{03}^{a} = A_{03}^{a}(\rho_{00} - \rho_{11}) + B_{03}^{a}(\rho_{11} - \rho_{22})$$
$$+ C_{03}^{a}(\rho_{22} - \rho_{33}) + D_{03}^{a}(\rho_{00} - \rho_{33}) ,$$

$$\tilde{\rho}_{03}^{b} = A_{03}^{b}(\rho_{00} - \rho_{11}) + B_{03}^{b}(\rho_{11} - \rho_{22})$$
$$+ C_{03}^{b}(\rho_{22} - \rho_{33}) + D_{03}^{b}(\rho_{00} - \rho_{33}) ,$$

where the coefficients are to be determined and where the diagonal element difference under the influence of the fields is also to be determined.

Using standard and graph algebraic approaches, the full set of coefficients have been determined. There are certain combinations of Rabi frequencies and detunings which appear often and merit new definitions of the following kind:

$$A = -\Lambda_{01}\Lambda_{32}(1/L_{03}^{a} + 1/T_{12}^{b}) ,$$

$$A' = -\Lambda_{10}\Lambda_{23}(1/L_{03}^{a} + 1/T_{12}^{b}) ,$$

$$B = -\Lambda_{12}\Lambda_{03}(1/T_{23}^{b} + 1/L_{10}^{a}) ,$$

$$B' = -\Lambda_{21}\Lambda_{30}(1/T_{23}^{b} + 1/L_{10}^{a}) ,$$

$$C = -\Lambda_{12}\Lambda_{03}(1/L_{32}^{a} + 1/T_{01}^{b}) ,$$

$$C' = -\Lambda_{21}\Lambda_{30}(1/L_{32}^{a} + 1/T_{01}^{b}) ,$$

$$D = -\Lambda_{01}\Lambda_{32}(1/L_{21}^{a} + 1/T_{30}^{b}) ,$$

$$D' = -\Lambda_{10}\Lambda_{23}(1/L_{21}^{a} + 1/T_{30}^{b}) ,$$

and

$$X_{13b} = R_{13}^{b} - \Lambda_{01}\Lambda_{10}/L_{03}^{a} - \Lambda_{23}\Lambda_{32}/T_{12}^{b}$$
$$- \Lambda_{12}\Lambda_{21}/T_{23}^{b} - \Lambda_{03}\Lambda_{30}/L_{10}^{a} ,$$

$$X_{02b} = R_{02}^{b} - \Lambda_{01}\Lambda_{10}/T_{12}^{b} - \Lambda_{12}\Lambda_{21}/T_{01}^{b}$$
$$- \Lambda_{23}\Lambda_{32}/L_{03}^{a} - \Lambda_{03}\Lambda_{30}/L_{32}^{a} ,$$

$$X_{20a} = R_{20}^{a} - \Lambda_{01}\Lambda_{10}/L_{21}^{a} - \Lambda_{12}\Lambda_{21}/L_{10}^{a}$$
$$- \Lambda_{23}\Lambda_{32}/T_{30}^{b} - \Lambda_{03}\Lambda_{30}/T_{23}^{b} ,$$

$$X_{31a} = R_{31}^{a} - \Lambda_{01}\Lambda_{10}/T_{30}^{b} - \Lambda_{12}\Lambda_{21}/L_{32}^{a}$$
$$- \Lambda_{23}\Lambda_{32}/L_{21}^{a} - \Lambda_{03}\Lambda_{30}/T_{01}^{b} .$$

The determinant of the coefficients of the conjugate of Eqs. (17)–(28) is expressed compactly in terms of these as

$$\Delta = 1 - CC'/(X_{31a}X_{02b}) - DD'/(X_{31a}X_{20a}) - BB'/(X_{20a}X_{13b}) - AA'/(X_{13b}X_{02b})$$

$$- C'D'BA/(X_{31a}X_{20a}X_{13b}X_{02b}) - CA'B'D/(X_{02b}X_{13b}X_{20a}X_{31a})$$

$$+ AA'DD'/(X_{02b}X_{13b}X_{31a}X_{20a}) + BB'CC'/(X_{02b}X_{13b}X_{31a}X_{20a}) .$$

Four of the off-diagonal elements can be used as generators of the other eight in Eqs. (17)–(28). These four are $\tilde{\rho}_{02}^{b}$, $\tilde{\rho}_{31}^{a}$, $\tilde{\rho}_{20}^{a}$, and $\tilde{\rho}_{13}^{b}$ which are found to have the following 16 coefficients:

$$A_{02}^{b} = (\Lambda_{10}\Lambda_{21}/L_{10}^{a})[BA/(X_{13b}X_{02b}) + DC/(X_{31a}X_{02b})]/(X_{20a}\Delta)$$

$$+ (-\Lambda_{10}\Lambda_{03}/L_{10}^{a})\{(A/X_{02b})[1 - DD'/(X_{31a}X_{20a})] + B'DC/(X_{20a}X_{31a}X_{02b})\}/(X_{13b}\Delta) ,$$

$$B_{02}^{b} = (\Lambda_{21}\Lambda_{32}/L_{21}^{a})\{(C/X_{02b})[1 - BB'/(X_{20a}X_{13b})]$$

$$+ D'BA/(X_{20a}X_{13b}X_{02b})\}/(X_{31a}\Delta) + (-\Lambda_{10}\Lambda_{21}/L_{21}^{a})$$

$$\times [BA/(X_{13b}X_{02b}) + DC/(X_{31a}X_{02b})]/(X_{20a}\Delta) ,$$

$$C_{02}^b = (\Lambda_{32}\Lambda_{03}/L_{32}^a)[1 - BB'/(X_{13b}X_{20a}) - DD'/(X_{31a}X_{20a})]/(X_{02b}\Delta)$$

$$+ (-\Lambda_{21}\Lambda_{32}/L_{32}^a)\{(C/X_{02b})[1 - BB'/(X_{20a}X_{13b})]$$

$$+ D'BA/(X_{20a}X_{13b}X_{02b})\}/(X_{31a}\Delta) ,$$

$$D_{02}^b = (-\Lambda_{10}\Lambda_{03}/L_{03}^a)\{(A/X_{02b})[1 - DD'/(X_{31a}X_{20a})]$$

$$+ B'DC/(X_{20a}X_{31a}X_{02b})\}/(X_{13b}\Delta) + (\Lambda_{32}\Lambda_{03}/L_{03}^a)$$

$$\times [1 - B'B/(X_{13b}X_{20a}) - DD'/(X_{20a}X_{31a})]/(X_{02b}\Delta) ,$$

$$A_{31}^a = (-\Lambda_{10}\Lambda_{03}/L_{10}^a)[AC'/(X_{02b}X_{31a}) + B'D/(X_{20a}X_{31a})]/(X_{13b}\Delta)$$

$$+ (\Lambda_{10}\Lambda_{21}/L_{10}^a)$$

$$\times \{(D/X_{31a})[1 - AA'/(X_{02b}X_{13b})] + BAC'/(X_{13b}X_{02b}X_{31a})\}/(X_{20a}\Delta) ,$$

$$B_{31}^a = (-\Lambda_{10}\Lambda_{21}/L_{21})\{(D/X_{31a})[1 - AA'/(X_{02b}X_{13b})] + BAC'/(X_{13b}X_{02b}X_{31a})\}/(X_{20a}\Delta) + (\Lambda_{21}\Lambda_{32}/L_{21}^a)$$

$$\times [1 - AA'/(X_{02b}X_{13b}) - BB'/(X_{13b}X_{20a})]/(X_{31a}\Delta) ,$$

$$C_{31}^a = (\Lambda_{32}\Lambda_{03}/L_{32}^a)\{(C'/X_{31a})[1 - BB'/(X_{13b}X_{20a})] + A'B'D/(X_{13b}X_{20a}X_{31a})\}/(X_{02b}\Delta) + (-\Lambda_{21}\Lambda_{32}/L_{32}^a)$$

$$\times [1 - AA'/(X_{02b}X_{13b}) - BB'/(X_{13b}X_{20a})]/(X_{31a}\Delta) ,$$

$$D_{31}^a = (-\Lambda_{10}\Lambda_{03}/L_{03}^a)[AC'/(X_{02b}X_{31a}) + B'D/(X_{20a}X_{31a})]/(X_{13b}\Delta) + (\Lambda_{32}\Lambda_{03}/L_{03}^a)$$

$$\times \{(C'/X_{31a})[1 - BB'/(X_{13b}X_{20a})] + A'B'D/(X_{13b}X_{20a}X_{31a})\}/(X_{02b}\Delta) ,$$

$$A_{20}^a = (-\Lambda_{10}\Lambda_{03}/L_{10}^a)\{(B'/X_{20a})[1 - C'C/(X_{02b}X_{31a})] + AC'D'/(X_{02b}X_{31a}X_{20a})\}/(X_{13b}\Delta) + (\Lambda_{10}\Lambda_{21}/L_{10}^a)$$

$$\times [1 - C'C/(X_{02b}X_{31a}) - AA'/(X_{02b}X_{13b})]/(X_{20a}\Delta) ,$$

$$B_{20}^a = (-\Lambda_{10}\Lambda_{21}/L_{21}^a)[1 - C'C/(X_{02b}X_{31a}) - AA'/(X_{02b}X_{13b})]/(X_{20a}\Delta) + (\Lambda_{21}\Lambda_{32}/L_{21}^a)$$

$$\times \{(D'/X_{20a})[1 - AA'/(X_{02b}X_{13b})] + CA'B'/(X_{02b}X_{13b}X_{20a})\}/(X_{31a}\Delta) ,$$

$$C_{20}^a = (\Lambda_{32}\Lambda_{03}/L_{32}^a)[C'D'/(X_{31a}X_{20a}) + A'B'/(X_{13b}X_{20a})]/(X_{02b}\Delta) + (-\Lambda_{21}\Lambda_{32}/L_{32}^a)$$

$$\times \{(D'/X_{20a})[1 - AA'/(X_{02b}X_{13b})] + CA'B'/(X_{02b}X_{13b}X_{20a})\}/(X_{31a}\Delta) ,$$

$$D_{20}^a = (-\Lambda_{10}\Lambda_{03}/L_{03}^a)\{(B'/X_{20a})[1 - C'C/(X_{02b}X_{31a})] + AC'D'/(X_{02b}X_{31a}X_{20a})\}/(X_{13b}\Delta) + (\Lambda_{32}\Lambda_{03}/L_{03}^a)$$

$$\times [C'D'/(X_{31a}X_{20a}) + A'B'/(X_{13b}X_{20a})]/(X_{02b}\Delta) ,$$

$$A_{13}^b = (-\Lambda_{10}\Lambda_{03}/L_{10}^a)[1 - C'C/(X_{31a}X_{02b}) - DD'/(X_{20a}X_{31a})]/(X_{13b}\Delta) + (\Lambda_{10}\Lambda_{21}/L_{10}^a)$$

$$\times \{(B/X_{13b})[1 - C'C/(X_{31a}X_{02b})] + D'CA/(X_{31a}X_{02b}X_{13b})\}/(X_{20a}\Delta) ,$$

$$B_{13}^b = (\Lambda_{21}\Lambda_{32}/L_{21}^a)[D'B/(X_{20a}X_{13b}) + CA'/(X_{02b}X_{13b})]/(X_{31a}\Delta) + (-\Lambda_{10}\Lambda_{21}/L_{21}^a)$$

$$\times \{(B/X_{13b})[1 - CC'/(X_{31a}X_{02b})] + DCA'/(X_{31a}X_{02b}X_{13b})\}/(X_{20a}\Delta) ,$$

$$C_{13}^b = (\Lambda_{32}\Lambda_{03}/L_{32}^a)\{(A'/X_{13b})[1 - DD'/(X_{31a}X_{20a})] + C'D'B/(X_{31a}X_{20a}X_{13b})\}/(X_{02b}\Delta) + (-\Lambda_{21}\Lambda_{32}/L_{32}^a)$$

$$\times [D'B/(X_{20a}X_{13b}) + CA'/(X_{02b}X_{13b})]/(X_{31a}\Delta) ,$$

$$D_{13}^b = (-\Lambda_{10}\Lambda_{03}/L_{03}^a)[1 - CC'/(X_{31a}X_{02b}) - DD'/(X_{31a}X_{20a})]/(X_{13b}\Delta) + (\Lambda_{32}\Lambda_{03}/L_{03}^a)$$

$$\times \{(A'/X_{13b})[1 - DD'/(X_{31a}X_{20a})] + C'D'B/(X_{31a}X_{20a}X_{13b})\}/(X_{02b}\Delta) .$$

Given these, the remaining 32 coefficients for the other eight off-diagonal elements are found to be

$$A_{01}^b = (\Lambda_{03}A_{31}^a - \Lambda_{21}A_{02}^b)/T_{01}^b , \quad A_{10}^a = (\Lambda_{10}/L_{10}^a) + (\Lambda_{12}A_{20}^a - \Lambda_{30}A_{13}^b)/L_{10}^a ,$$

$$B_{01}^b = (\Lambda_{03}B_{31}^a - \Lambda_{21}B_{02}^b)/T_{01}^b , \quad B_{10}^a = (\Lambda_{12}B_{20}^a - \Lambda_{30}B_{13}^b)/L_{10}^a ,$$

$$C_{01}^b = (\Lambda_{03}C_{31}^a - \Lambda_{21}C_{02}^b)/T_{01}^b , \quad C_{10}^a = (\Lambda_{12}C_{20}^a - \Lambda_{30}C_{13}^b)/L_{10}^a ,$$

$$D_{01}^b = (\Lambda_{03}D_{31}^a - \Lambda_{21}D_{02}^b)/T_{01}^b , \quad D_{10}^a = (\Lambda_{12}D_{20}^a - \Lambda_{30}D_{13}^b)/L_{10}^a ,$$

$$A_{12}^{b} = (\Lambda_{10}A_{02}^{b} - \Lambda_{32}A_{13}^{b})/T_{12}^{b}, \quad A_{21}^{a} = (\Lambda_{23}A_{31}^{a} - \Lambda_{01}A_{20}^{a})/L_{21}^{a} ,$$

$$B_{12}^{b} = (\Lambda_{10}B_{02}^{b} - \Lambda_{32}B_{13}^{b})/T_{12}^{b}, \quad B_{21}^{a} = (\Lambda_{21}/L_{21}^{a}) + (\Lambda_{23}B_{31}^{a} - \Lambda_{01}B_{20}^{a})/L_{21}^{a} ,$$

$$C_{12}^{b} = (\Lambda_{10}C_{02}^{b} - \Lambda_{32}C_{13}^{b})/T_{12}^{b}, \quad C_{21}^{a} = (\Lambda_{23}C_{31}^{a} - \Lambda_{01}C_{20}^{a})/L_{21}^{a} ,$$

$$D_{12}^{b} = (\Lambda_{10}D_{02}^{b} - \Lambda_{32}D_{13}^{b})/T_{12}^{b}, \quad D_{21}^{a} = (\Lambda_{23}D_{31}^{a} - \Lambda_{01}D_{20}^{a})/L_{21}^{a} ,$$

$$A_{23}^{b} = (\Lambda_{21}A_{13}^{b} - \Lambda_{03}A_{20}^{a})/T_{23}^{b}, \quad A_{32}^{a} = (\Lambda_{30}A_{02}^{b} - \Lambda_{12}A_{31}^{a})/L_{32}^{a} ,$$

$$B_{23}^{b} = (\Lambda_{21}B_{13}^{b} - \Lambda_{03}B_{20}^{a})/T_{23}^{b}, \quad B_{32}^{a} = (\Lambda_{30}B_{02}^{b} - \Lambda_{12}B_{31}^{a})/L_{32}^{a} ,$$

$$C_{23}^{b} = (\Lambda_{21}C_{13}^{b} - \Lambda_{03}C_{20}^{a})/T_{23}^{b}, \quad C_{32}^{a} = (\Lambda_{32}/L_{32}^{a}) + (\Lambda_{30}C_{02}^{b} - \Lambda_{12}C_{31}^{a})/L_{32}^{a} ,$$

$$D_{23}^{b} = (\Lambda_{21}D_{13}^{b} - \Lambda_{03}D_{20}^{a})/T_{23}^{b}, \quad D_{32}^{a} = (\Lambda_{30}D_{02}^{b} - \Lambda_{12}D_{31}^{a})/L_{32}^{a} ,$$

$$A_{30}^{b} = (\Lambda_{32}A_{20}^{a} - \Lambda_{10}A_{31}^{a})/T_{30}^{b}, \quad A_{03}^{a} = (\Lambda_{01}A_{13}^{b} - \Lambda_{23}A_{03}^{b})/L_{03}^{a} ,$$

$$B_{30}^{b} = (\Lambda_{32}B_{20}^{a} - \Lambda_{10}B_{31}^{a})/T_{30}^{b}, \quad B_{03}^{a} = (\Lambda_{01}B_{13}^{b} - \Lambda_{23}B_{02}^{b})/L_{03}^{a} ,$$

$$C_{30}^{b} = (\Lambda_{32}C_{20}^{a} - \Lambda_{10}C_{31}^{a})/T_{30}^{b}, \quad C_{03}^{a} = (\Lambda_{01}C_{13}^{b} - \Lambda_{23}C_{02}^{b})/L_{03}^{a} ,$$

$$D_{30}^{b} = (\Lambda_{32}D_{20}^{a} - \Lambda_{10}D_{31}^{a})/T_{30}^{b}, \quad D_{03}^{a} = (-\Lambda_{03}/L_{03}^{a}) + (\Lambda_{01}D_{13}^{b} - \Lambda_{23}D_{02}^{b})/L_{03}^{a} .$$

Because ρ is Hermitian, the 12 conjugate off-diagonal elements follow automatically.

The next stage entails the determination of the saturated diagonal elements. Since all interesting multiphoton spectroscopy is contained in the above coefficients, we only outline the steps used to proceed with this part. As an illustration, one driving term for ρ_{00} in Eq. (7) is $(\rho_{01}-\rho_{10})\mu_{10}\cdot E/\hbar$, which, with the help of Eq. (29), becomes

$$2\,\mathrm{Im}(\tilde{\rho}_{10}^{a}\Lambda_{10}+\tilde{\rho}_{10}^{b}\Lambda_{10}F) = 2\,\mathrm{Im}\{\Lambda_{10}[(A_{01}^{a}+FA_{01}^{b})(\rho_{00}-\rho_{11})+(B_{01}^{a}+FB_{01}^{b})(\rho_{11}-\rho_{22})$$

$$+(C_{01}^{a}+FC_{01}^{b})(\rho_{22}-\rho_{33})+(D_{01}^{a}+FD_{01}^{b})(\rho_{00}-\rho_{33})]\}$$

$$= Q_1(\rho_{00}-\rho_{11})+Q_2(\rho_{11}-\rho_{22})+Q_3(\rho_{22}-\rho_{33})+Q_4(\rho_{00}-\rho_{33}) ,$$

where the Q_1 are constants and can be most easily evaluated numerically along with the saturated value of the diagonal elements. The actual value of the off-diagonal element then follows from the above coefficients and the saturated value of the diagonal elements. As a convenience to the interested reader, we list below the equivalents to

Eqs. (37) and (39) for the remaining three waves. The following table lists the substitutions which are used to transform the equations so that they are appropriate to one of the other three waves, when it is weak (A, B, C, and D are Λ_{01}, Λ_{12}, Λ_{23}, and Λ_{03}, respectively):

$\Lambda_{03}\rightarrow0$ ρ_{03}^{b}	$\Lambda_{01}\rightarrow0$ ρ_{01}^{b}	$\Lambda_{12}\rightarrow0$ ρ_{12}^{b}	$\Lambda_{23}\rightarrow0$ ρ_{23}^{b}	$\Lambda_{03}\rightarrow0$ ρ_{03}^{a}	$\Lambda_{01}\rightarrow0$ ρ_{01}^{a}	$\Lambda_{12}\rightarrow0$ ρ_{12}^{a}	$\Lambda_{23}\rightarrow0$ ρ_{23}^{a}
A	D	A^{*}	B^{*}	A	D	A	B
B	C^{*}	D	A^{*}	B	C	D	A
C	B^{*}	C^{*}	D	C	B	C	D
ρ_{00}	ρ_{00}	ρ_{11}	ρ_{22}	D	A	B	C
ρ_{11}	ρ_{33}	ρ_{00}	ρ_{11}	ρ_{00}	ρ_{00}	ρ_{11}	ρ_{22}
ρ_{22}	ρ_{22}	ρ_{33}	ρ_{00}	T_{01}^{b}	T_{03}^{b}	T_{10}^{b}	T_{21}^{b}
ρ_{33}	ρ_{11}	ρ_{22}	ρ_{33}	T_{12}^{b}	T_{32}^{b}	T_{03}^{b}	T_{10}^{b}
L_{01}^{a}	L_{03}^{a}	L_{10}^{a}	L_{21}^{a}	T_{23}^{b}	T_{21}^{b}	T_{32}^{b}	T_{03}^{b}
L_{12}^{a}	L_{32}^{a}	L_{03}^{a}	L_{10}^{a}	R_{02}^{b}	R_{02}^{a}	R_{13}^{a}	R_{20}^{b}
L_{23}^{a}	L_{21}^{a}	L_{32}^{a}	L_{03}^{a}	R_{13}^{b}	R_{31}^{b}	R_{02}^{a}	R_{13}^{a}
R_{02}^{b}	R_{02}^{b}	R_{13}^{b}	R_{20}^{a}	L_{03}^{a}	L_{01}^{a}	L_{12}^{a}	L_{23}^{a}
R_{13}^{a}	R_{31}^{a}	R_{02}^{b}	R_{13}^{b}				
T_{03}^{b}	T_{01}^{b}	T_{12}^{b}	T_{23}^{b}				

*Permanent address: Institut d'Électronique Fondamentale, Université de Paris–Sud, 91405 Orsay Cédex, France.

[1]J. F. Ward, Rev. Mod. Phys. **37**, 1 (1965), J.-L. Oudar and Y. R. Shen, Phys. Rev. A **22**, 1141 (1980).

[2]C. R. Vidal, Appl. Opt. **19**, 3897 (1980).

[3]H. Puell, H. Scheingraber, and C. R. Vidal, Phys. Rev. A **22**, 1165 (1980).

[4]J. J. Wynne and P. P. Sorokin, in *Nonlinear Infrared Generation,* edited by Y.-R. Shen (Springer, New York, 1977), pp. 159–214.

[5]R. Frey, F. Pradere, and J. Ducing, Opt. Commun. **23**, 65 (1977).

[6]B. G. Danly, S. G. Evangelides, R. J. Temkin, and B. Lax, in *Infrared and Millimeter Waves,* edited by K. J. Button (Academic, New York, 1984), Vol. 12, pp. 195–278.

[7]For an example of third-harmonic generation in two-level systems, see D. P. Akitt and P. D. Coleman, J. Appl. Phys. **36**, 2004 (1965).

[8]A. O. Melikyan and S. G. Saakyan, Zh. Eksp. Teor. Fiz. **76**, 1530 (1978) [Sov. Phys.—JETP **49**, 776 (1979)]; and, more recently, M. P. Sharma and J. A. Roversi, Phys. Rev. A **29**, 3264 (1984).

[9]S. J. Petuchowski, J. D. Oberstar, and T. A. DeTemple, Phys. Rev. A **20**, 529 (1979).

[10]M. Tsukakoshi, Jpn. J. Appl. Phys. **21**, L417 (1982).

[11]Y. K. Lin and D. Gong, Acta Opt. Sin. **2**, 210 (1982).

[12]B. Dick and R. M. Hochstrasser, Chem. Phys. **75**, 133 (1983).

[13]F. Julien, P. Wazen, J.-M. Lourtioz, T. A. DeTemple, and S. J. Petuchowski, Opt. Commun. **54**, 246 (1985); and also M. Bernardini, M. Giorgi, and S. Marchetti, Int. J. Infrared Millimiter Waves **8**, 699 (1987).

[14]A. M. Levine, N. Chencinski, W. M. Schreiber, A. N. Weiszmann, and Y. Prior, Phys. Rev. A **35**, 2550 (1987).

[15]C.-Y. Tai, C. C. Kim, R. T. Deck, and Y.-T. Wu, Phys. Rev.

A **33**, 3970 (1986).

[16]T. A. DeTemple, L. A. Bahler, and J. Osmundson, Phys. Rev. A **24**, 1959 (1981).

[17]F. Julien, J.-M. Lourtioz, and T. A. DeTemple (unpublished).

[18]S. J. Petuchowski and T. A. DeTemple, Opt. Lett. **5**, 227 (1981).

[19]H. K. Chung and T. A. DeTemple, Phys. Rev. A **22**, 2647 (1980).

[20]T. A. DeTemple, S. J. Petuchowski, and H. K. Chung, Phys. Rev. A **22**, 2636 (1980).

[21]T. K. Yee and T. K. Gustafson, Phys. Rev. A **18**, 1597 (1978).

[22]This result may be applied to any of the other three waves shown in Fig. 1 by the following steps. (i) Since only the square of the Rabi frequency appears in the Stark-shift terms, $\Lambda_{ij}^2 = \Lambda_{ij}\Lambda_{ij}^*$. (ii) Identify the complex detunings and hence the sign of the phase in the Rabi frequency. (iii) Use Eqs. (37) and (39) for ω_4 and the substitutions listed in the Appendix, which will transform these so that they are appropriate to the other three waves, when weak.

[23]For the other two linkage diagrams of Fig. 1, Eq. (38) is transformed as follows. For Fig. 1(b), $Z = \Omega_{23} - \omega_3$ and the symbol Z in Eq. (38) is to be replaced by $-Z$. For Fig. 1(c), $Y = \Omega_{12} - \omega_2$ and the symbol Y in Eq. (38) is to be replaced by $-Y$.

[24]The second-harmonic polarization will exist only if μ_{02} or μ_{13} is nonzero, which can only occur in a mixed-parity system.

[25]K. S. Yngvesson and E. L. Kollberg, Appl. Phys. Lett. **36**, 104 (1980).

[26]F. Julien, P. Wazen, J.-M. Lourtioz, and T. A. DeTemple, J. Phys. (Paris) **47**, 781 (1986).

[27]C.-X. Wang, R.-W. Wang, and E.-S. Fu, Opt. Commun. **64**, 437 (1987).

[28]C.-Y. Tai, R. T. Deck, and C. Kim, Phys. Rev. A **37**, 163 (1988).